PROCEEDINGS of
CHEF 2013

Characteristics of hadronic showers in the CALICE AHCAL

Marina Chadeeva*, **on behalf of the CALICE Collaboration**
Institute for Theoretical and Experimental Physics, Moscow, Russia
E-mail: marina@itep.ru

The experimental data obtained with the high-granular CALICE analogue hadronic calorimeter provides valuable input to the validation of the shower models used for Monte Carlo simulations. The calorimeter response, resolution and characteristics of longitudinal and radial shower development are analysed for initial particle momenta 10–80 GeV and compared with the predictions of different GEANT4 physics lists. Most of the studied physics lists predict steeper energy dependence of the calorimeter response for pions and underestimate the mean radial width of hadronic shower. The calorimeter response to pion-induced showers is observed to be higher than that for protons, which can be largely explained by the difference in available energy for mesons and baryons. The spatial parameters of proton-induced showers, such as mean longitudinal depth and mean shower radius, are larger than those of pion-induced showers by $\sim$5% and $\sim$10%, respectively. The biggest discrepancy between test beam data and predictions of the physics lists from GEANT4 version 9.4 amounts up to $\sim$10% and concerns the underestimation of the calorimeter response for pions at 10 GeV and mean shower radius in all studied energy range.

Calorimetry for High Energy Frontiers - CHEF 2013,
April 22-25, 2013
Paris, France

*Speaker.

1. Introduction

One of the key factors to achieve an unprecedented detector performance in the future lepton collider experiments is a high granularity of calorimeters, which allows an application of the Particle Flow Approach [1]. Since 2006 several CALICE high-granular calorimeter prototypes equipped with different readout systems and absorber materials (steel or tungsten) have been exposed to electron and hadron test beams at DESY, CERN and FNAL with initial particle momenta from 1 to 130 GeV/c. The main goals of these experimental efforts were to estimate the calorimeter response and resolution and study spatial characteristics of hadronic showers to provide a validation of the shower models used for Monte Carlo simulations. The quality of predictions of spatial shower development is important for reliable estimates of the jet energy resolution. The longitudinal depth defines a shower containment in the calorimeter while the radial size of hadronic shower is a key factor for the PFA efficiency that depends on the ability to disentangle showers induced by charged and neutral hadrons.

The presented results are based on the data taken with the CALICE analogue scintillator-steel hadronic calorimeter with SiPM readout (AHCAL) exposed to positive hadrons with momenta from 10 to 80 GeV/c. The effective nuclear interaction length, calorimeter response and resolution, longitudinal and radial characteristics of proton and pion-induced showers are compared. The comparison is also performed with simulations using five physics lists from GEANT4 version 9.4.

2. Test beam data and simulations

The CALICE setup used during CERN 2007 test beam campaign is described in detail in [2] and shown in Fig. 1. It comprised the Si-W electromagnetic calorimeter (ECAL) [3], the AHCAL [4] and tail catcher and muon tracker (TCMT) [5]. The positive pion beams in the momentum range from 30 to 80 GeV/c were delivered from CERN SPS H6 beam line. The data below 20 GeV/c were taken at FNAL with the setup without ECAL, which is described in [6]. The AHCAL comprises 38 plates of 16 mm-thick steel absorber interleaved with active layers assembled from 5 mm-thick scintillator tiles (3×3, 6×6 and 12×12 cm^2) with individual SiPM readout. The longitudinal depth of calorimeter prototypes is $\sim$1, $\sim$5.3, and $\sim$5.5 effective nuclear interaction lengths for ECAL, AHCAL, and TCMT, respectively.

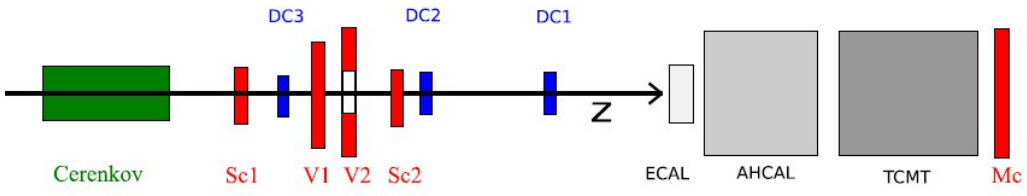

Figure 1: CALICE setup (not to scale) during CERN 2007 test beam campaign. Sc, V, Mc and DC stand for scintillator triggers, beam veto counters, muon veto counter, and tracking drift chambers, respectively. Test beam enters from the left along Z.

The hadron test beam is usually a mixture of different particles: hadrons, muons, electrons, which are separated off-line during data analysis. The event selection procedure involves informa-

tion from Čerenkov counter and TCMT, estimates of some spatial shower parameters and identification of the position of the first inelastic interaction (see [2, 7] for details). The remaining admixture of muons and positrons in the selected hadron samples is less than 0.5% and 1% respectively. The off-line event-by-event separation of pions and protons was performed using information from the Čerenkov counter placed upstream of the calorimeter setup. The proton sample purity was estimated basing on the Čerenkov counter efficiency and varies from ∼65% at 10 GeV to ∼95% at 30 GeV. The contamination of the analysed samples is taken into account in the systematic uncertainties of the studied observables.

The dedicated algorithm of identification of the shower start (first inelastic interaction) position, which is tuned using simulated pion samples, allows to estimate the effective nuclear interaction length that was found to be ∼20% lower for protons than for pions and is in good agreement with the values extracted from PDG data [8]. To reduce the fraction of remaining positrons in the samples taken without ECAL and to minimise the leakage into TCMT, only events with the shower start in the third, fourth and fifth AHCAL layers are used in the analysis of calorimeter response, energy resolution and spatial characteristics of hadronic showers.

The simulations were performed using the Mokka environment as an interface to GEANT4 version 9.4 patch 3 accompanied by the digitisation procedure that includes the simulation of SiPM response, noise contribution and light crosstalk between scintillator tiles. Five physics lists were studied: QGSP_BERT, QBBC, CHIPS, FTFP_BERT, and FTF_BIC [9, 10].

3. Calorimeter response and resolution

The visible signal in each calorimeter cell is obtained in units of minimum ionising particle (MIP) as described in [4]. Only cells with the signal above 0.5 MIP were considered for analysis and are called hits. The reconstructed energy E_{event} in units of GeV for selected events with track in ECAL is calculated from the visible signal measured in different detector sections by multiplication with suitable calibration factors:

$$E_{\text{event}} = \sum_{k=1}^{3} v \cdot k \cdot M_k^{\text{ECAL}} + \frac{e}{\pi} \cdot w \left(M^{\text{AHCAL}} + M_1^{\text{TCMT}} + 5 \cdot M_2^{\text{TCMT}} \right), \tag{3.1}$$

where $v = 0.00295$ GeV/MIP is the conversion factor for track in ECAL obtained with muons; $w = 0.02364$ GeV/MIP is the conversion factor obtained from electromagnetic calibration of AHCAL [11]; M^{ECAL}, M^{AHCAL}, and M^{TCMT} are the sums of visible signals in the corresponding calorimeter subsections; $\frac{e}{\pi} = 1.2$ is the scaling coefficient to take into account a different response to electrons and hadrons in the non-compensating AHCAL (the coefficient was obtained for pions by averaging the ratio of beam energy to the total energy reconstructed at electromagnetic scale over the studied energy range). The reconstructed energy distributions are fitted with a Gaussian in the interval of ±2 RMS around the mean value. The parameters of this Gaussian fit at a given beam energy are referred to as the mean reconstructed energy E_{reco} and resolution σ_{reco}, respectively.

The AHCAL response for charged pions was observed to be linear within ±2% in the energy range 10–80 GeV in [2]. The difference in calorimeter response for pions and protons increases with decreasing initial particle energy and can be largely explained by the baryon conservation law that results in lower probability to produce leading baryon in pion interaction with nucleus [12, 13].

The so called "available energy" corresponds to the total particle energy in case of mesons and to the kinetic energy of a particle in case of baryons:

$$E^{\text{pion}}_{\text{available}} = \sqrt{p^2_{\text{beam}} + m^2_{\text{pion}}}, \qquad E^{\text{proton}}_{\text{available}} = \sqrt{p^2_{\text{beam}} + m^2_{\text{proton}}} - m_{\text{proton}}, \tag{3.2}$$

where p_{beam} is a beam momentum and m_{pion} (m_{proton}) is the pion (proton) rest mass.

Figure 2 shows the relative residuals both to beam momentum (left) and to available energy (right) for data and QGSP_BERT physics list for positive pions and protons. If the available energy is considered, the difference between positive pion and proton response remains $\leq$4%, that is in agreement with the difference observed for Sc-Fe Tile ATLAS calorimeter [14]. The Fritiof-based physics lists show a similar behaviour and give very good predictions for protons above 20 GeV.

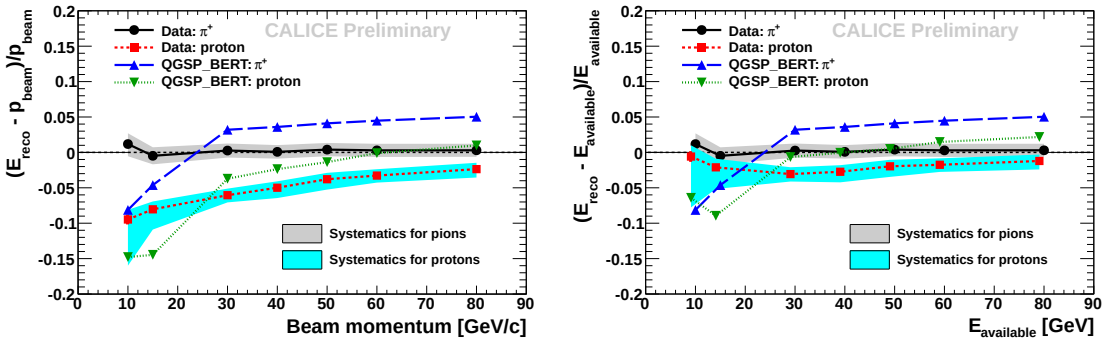

Figure 2: Relative residuals of reconstructed energy E_{reco} to beam momentum (left) and available energy (right) for test beam data (black circles for pions and red squares for protons) and QGSP_BERT physics list (blue triangles for pions and green down triangles for protons). Systematic uncertainties for data are shown with grey band for pions and cyan band for protons.

The fractional energy resolution for hadrons in test beam data is well described by the three-component function, including stochastic ($\sim \frac{58\%}{\sqrt{E/\text{GeV}}}$), constant (~1.6%) and noise ($\sim \frac{0.18}{E/\text{GeV}}$) contributions [2], a good agreement being observed between pions and protons. The best prediction of the fractional resolution is given by QGSP_BERT physics list in all studied energy range.

4. Longitudinal and radial shower parameters

The studied longitudinal parameter $Z0$ is a centre of gravity of a shower along beam direction. The value of $Z0$ for each event is calculated as follows:

$$Z0 = \frac{\sum_{i=1}^{N_{\text{sh}}} e_i \cdot (z_i - z_{\text{start}})}{\sum_{i=1}^{N_{\text{sh}}} e_i}, \tag{4.1}$$

where N_{sh} is the number of hits in AHCAL from shower start layer and beyond, e_i is the hit energy, z_i is the distance from hit layer to the calorimeter front and z_{start} is the distance from shower start layer to the calorimeter front face. The important feature of the observable $Z0$ is its independence on the distribution of shower start position that allows to compare longitudinal shower development

for different types of hadrons. The typical distribution of the longitudinal centre of gravity $Z0$ for pion-induced showers is shown in Fig. 3(left).

The radial shower development can be characterised by a shower radius, i.e. an energy weighted sum of hit radial distances to the shower axis (in the plane perpendicular to the beam direction):

$$R = \frac{\sum_{i=1}^{N_{\rm sh}} e_i \cdot r_i}{\sum_{i=1}^{N_{\rm sh}} e_i}, \tag{4.2}$$

where $N_{\rm sh}$ is the number of hits in AHCAL from shower start layer and beyond, e_i is the hit energy, $r_i = \sqrt{(x_i - x_0)^2 + (y_i - y_0)^2}$ is the distance from hit with coordinates (x_i,y_i) to shower axis with coordinates (x_0,y_0). The shower axis is defined using primary track coordinates in ECAL or event centre of gravity for the runs without ECAL. The typical distribution of the shower radius R for pions is shown in Fig. 3(right).

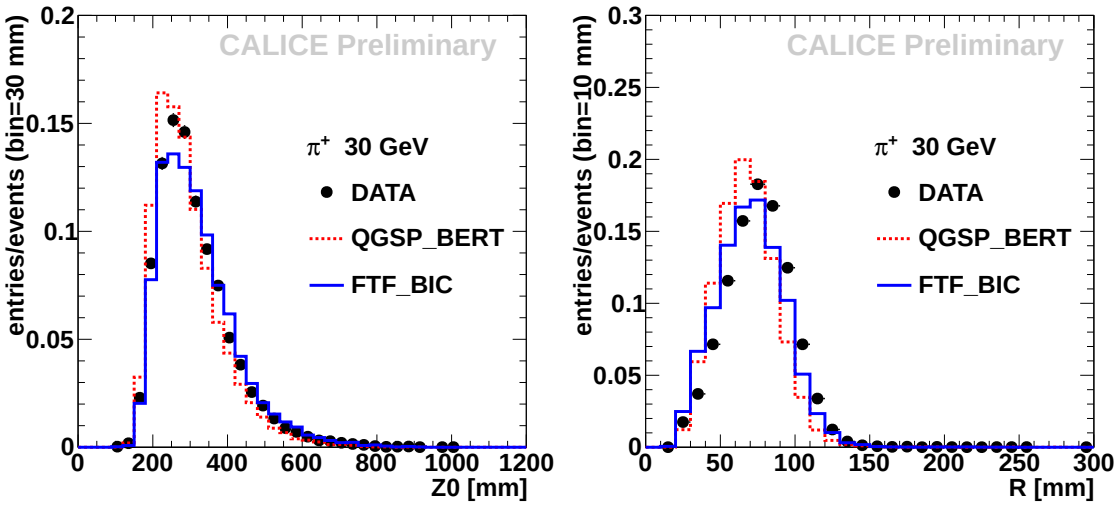

Figure 3: Distributions of longitudinal centre of gravity (left) and shower radius (right) of hadronic showers initiated by pions with initial momentum of 30 GeV/c for test beam data (black circles) and QGSP_BERT (red dashed line) and FTF_BIC (blue solid line) physics lists.

The mean longitudinal shower depth $\langle Z0 \rangle$ extracted from the distributions of $Z0$ increases logarithmically with energy. Figure 4 shows the ratios of simulations to data. The QGSP_BERT physics list gives the best predictions for both pions and protons below 20 GeV. The QGSP_BERT, QBBC and CHIPS physics lists underestimate $\langle Z0 \rangle$ by ∼4-8% for both pions and protons above 20 GeV. The FTFP_BERT and FTF_BIC physics lists give a very good prediction of $\langle Z0 \rangle$ for pions above 40 GeV and overestimate this value for protons by ∼5%.

The mean shower radius $\langle R \rangle$ is extracted from the distributions like those shown in Fig. 3(right). $\langle R \rangle$ decreases logarithmically with increasing energy and this behaviour is well reproduced by all studied physics lists. The pion (proton) showers are observed to be narrower by ∼25% (∼30%) at 80 GeV than at 10 GeV. This is explained by the increase of electromagnetic fraction in hadronic shower, since electromagnetic sub-showers tend to be more compact. The ratio of simulations to data is shown in Fig. 5. The best prediction of shower radius for pions is given by the CHIPS

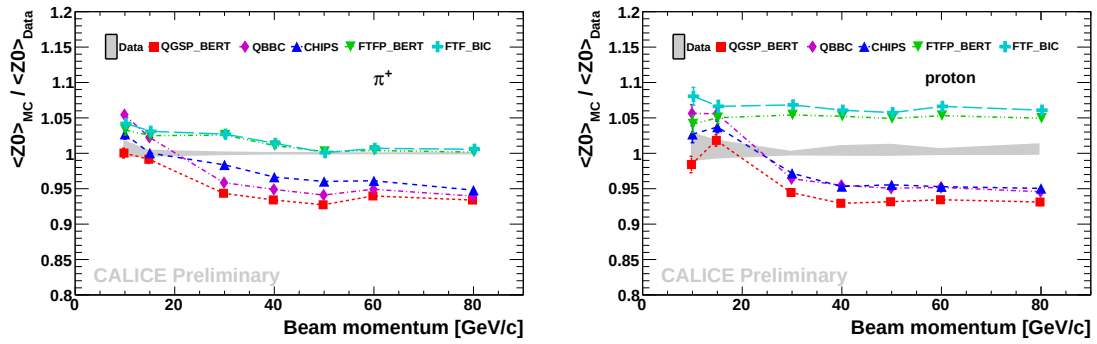

Figure 4: Ratio of the mean longitudinal centre of gravity of hadronic shower extracted from simulations to that extracted from data versus beam momentum for pion-induced (left) and proton-induced showers (right). Systematic uncertainties for data are shown with grey band.

physics list while other physics lists underestimate $\langle R \rangle$ by $\sim$10%. For protons, all physics lists, except for CHIPS, coincide with data within uncertainties at 10 GeV and the best prediction in the studied energy range is given by FTF_BIC physics list (within $\sim$2%).

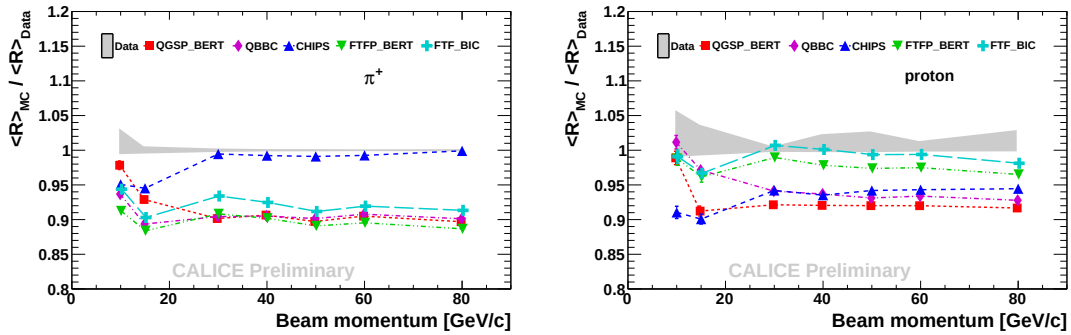

Figure 5: Ratio of the mean radial shower width extracted from simulations to that extracted from data versus beam momentum for pion-induced (left) and proton-induced showers (right). Systematic uncertainties for data are shown with grey band.

5. Conclusion

The parameters of hadronic showers in the CALICE analogue scintillator-steel hadronic calorimeter were studied using test beam data collected at CERN and FNAL for beams of positive hadrons with initial momenta from 10 to 80 GeV/c. The calorimeter response, resolution and spatial characteristics of shower development were compared with GEANT4 simulations performed with five physics lists from version 9.4: QGSP_BERT, QBBC, CHIPS, FTFP_BERT and FTF_BIC.

All studied GEANT4 physics lists predict steeper behaviour of pion response than is observed in data. The deficiency of calorimeter response for protons comparing to that for pions, which cannot be explained by the difference in available energy, is found to be $\sim$2–4%. The best prediction

of the fractional resolution for both pions and protons is given by QGSP_BERT physics list in the analysed energy range.

The longitudinal shower depth increases logarithmically with energy and is $\sim$5% lower for pions than for protons. The mean shower radius decreases logarithmically with increasing energy and is $\sim$10% lower for pions than for protons. Most physics lists underestimate the mean shower radius for both pions and protons by $\sim$6–10%, except for CHIPS that is in good agreement with pion data above 20 GeV and FTF_BIC physics list that predicts mean shower radius for protons with $\sim$2% accuracy.

References

[1] M. Thomson. Particle flow calorimetry and the PandoraPFA Algorithm. *NIM*, A611:25–40, 2009.

[2] C. Adloff et al. Hadronic energy resolution of a highly granular scintillator-steel calorimeter using software compensation techniques. *JINST*, 7:P09017, 2012.

[3] C. Adloff et al. Design and electronics commissioning of the physics prototype of a Si-W electromagnetic calorimeter for the International Linear Collider. *JINST*, 3:P08001, 2008.

[4] C. Adloff et al. Construction and Commissioning of the CALICE Analog Hadron Calorimeter Prototype. *JINST*, 5:P05004, 2010.

[5] C. Adloff et al. Construction and performance of a silicon photomultiplier/extruded scintillator tail-catcher and muon-tracker. *JINST*, 7:P04015, 2012.

[6] N. Feege. Low-energetic hadron interactions in a highly granular calorimeter. *DESY-THESIS-2011-048*, 2011.

[7] The CALICE Collaboration. Pion and proton showers in the CALICE scintillator-steel AHCAL: comparison of global observables. *CALICE Analysis Note CAN-040*, 2013.

[8] J. Beringer et al. The Review of Particle Physics. *Phys.Rev.*, D86:010001, 2012.

[9] S. Agostinelli et al. GEANT4: A Simulation toolkit. *NIM*, A506:250, 2003.

[10] A. Ribon et al. Status of GEANT4 hadronic physics for the simulation of LHC experiments at the start of LHC physics program. *CERN-LCGAPP-2010-002*, 2010.

[11] C. Adloff et al. Electromagnetic response of a highly granular hadronic calorimeter. *JINST*, 6:P04003, 2011.

[12] T. A. Gabriel et al. Energy dependence of hadronic activity. *NIM*, A338:336–347, 1994.

[13] N. Akchurin et al. On the differences between high-energy proton and pion showers and their signals in a non-compensating calorimeter. *NIM*, A408:380–396, 1998.

[14] P. Adragna et al. Measurement of pion and proton response and longitudinal shower profiles up to 20 nuclear interaction lengths with the ATLAS Tile calorimeter. *NIM*, A615:158–181, 2010.